Dalton Transactions

ROYAL SOCIETY OF CHEMISTRY

PAPER

View Article Online
View Journal | View Issue

Cite this: *Dalton Trans.*, 2024, **53**, 16861

Aminophosphine PN^H complexes of Mn(I), Fe(II), and Co(II) and evaluation of their activities in the transfer hydrogenation of nitriles†

Ainur Slamova,‡[a] Ayazhan Bizhanova,‡[a] Ofeliya Talimonyuk,‡[a] Kristina A. Gudun,[a] Samat Tussupbayev,[b] Anton Dmitrienko,[c] Aishabibi Kassymbek,[a] Konstantin A. Lyssenko[d] and Andrey Y. Khalimon *[a]

Received 28th August 2024,
Accepted 26th September 2024

DOI: 10.1039/d4dt02442g

rsc.li/dalton

A series of Mn(I), Fe(II), and Co(II) complexes with PN^H ligands bearing secondary amine functionality were prepared and tested in the catalytic transfer hydrogenation of nitriles using ammonia borane as a hydrogen source. Among all tested complexes, a tetracoordinate Fe(II) bromide, (PN^H)FeBr$_2$, proved the most effective, representing a rare example of a highly active iron-based catalytic system for transfer hydrogenation reactions beyond carbonyl compounds and the first example of the iron catalyst for the transfer hydrogenation of nitriles to the corresponding primary amines. Mechanistic studies point out a metal–ligand cooperative mechanism enabled by the secondary amine moiety of the PN^H ligand.

Introduction

Catalytic transfer hydrogenation (TH) reactions have become an indispensable tool in synthetic organic chemistry, offering several advantages in safety, selectivity, and investment costs of transformations compared to stoichiometric reductions with metal hydride reagents and hydrogenations with compressed hydrogen gas.[1,2] Initially developed for precious metal catalysts (mostly Ru, but also Rh, Ir, *etc.*), TH reactions have found widespread applications in the reduction of carbonyl compounds to alcohols (including asymmetric variants), mainly due to the availability of various hydrogen sources, operational simplicity, and mild reaction conditions.[1,3] During the past decades, numerous 3d metal (so-called base metals, such as Mn, Fe, Co, and Ni) catalysts have been extensively studied as more economical surrogates to precious metal systems for TH of carbonyl compounds.[1*i–k*] In contrast, the analogous base-metal-catalyzed TH of unsaturated N-containing molecules is developed to a lesser extent.[1*k*] For instance, although nitriles are considered convenient precursors to amines, examples of efficient base metal catalysts for selective and mild TH of nitriles to the corresponding primary amines are scarce.[4] Only several reports on Co-[4*a*] and Mn-catalyzed[4*b–d*] transformations have been recently disclosed (Scheme 1). In contrast, despite their widespread applications in the TH of carbonyl compounds,[1*f,h,i,k*] no Fe catalysts for the TH of nitriles to primary amines have been reported. Nonetheless, such systems are highly

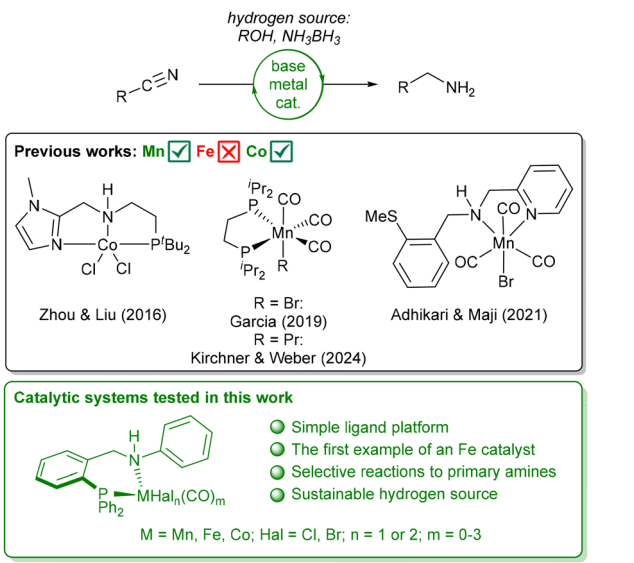

Scheme 1 Catalytic TH of nitriles to primary amines.

[a]*Department of Chemistry, School of Sciences and Humanities, Nazarbayev University, 53 Kabanbay Batyr Avenue, Astana 010000, Kazakhstan. E-mail: andrey.khalimon@nu.edu.kz*
[b]*Institute of Polymer Materials and Technologies, 3/1 Atyrau-1, Almaty 050019, Kazakhstan*
[c]*Department of Chemistry and Biochemistry, University of Windsor, 401 Sunset Avenue, Windsor, Ontario N9B 3P4, Canada*
[d]*Department of Chemistry, Lomonosov Moscow State University, Leninskie Gory 1-3, Moscow 119991, Russia*

†Electronic supplementary information (ESI) available: Complete experimental, spectroscopic, and computational details. CCDC 2379898, 2379897, 2380140 and 2379985 for **1-Mn**, **1-Fe**, **1-Co**, and **2-Co**. For ESI and crystallographic data in CIF or other electronic format see DOI: https://doi.org/10.1039/d4dt02442g

‡These authors contributed equally.

desirable, considering the high natural abundance and low toxicity of iron[1h] and the widespread synthetic utility of amines in the specialty chemicals industry.[5] With this in mind, we aimed to explore the chemistry of a series of structurally related base metal (Mn, Fe, and Co) complexes bearing easily accessible bidentate aminophosphine PN^H ligands and investigate their comparative catalytic activities in the TH of nitriles to the corresponding primary amines (Scheme 1). Herein we report our findings, including the development of the first example of a readily accessible Fe(II) catalytic system for the TH of nitriles. The reactions utilize ammonia borane (AB) as a hydrogen source and apply to a wide range of substrates, can be performed under mild conditions, and do not require the use of a base co-catalyst. Mechanistic studies suggest a metal–ligand cooperative route for TH reaction enabled by the proton transfer from the aminophosphine PN^H ligand.

Results and discussion

Preparation of PN complexes of Mn, Fe, and Co

The synthesis of $(PN^H)MnBr(CO)_3$ (**1-Mn**), $(PN^H)FeBr_2$ (**1-Fe**), and $(PN^H)CoCl_2$ (**1-Co**) is shown in Scheme 2. The aminophosphine PN^H ligand **1** was prepared by a straightforward reductive amination of 2-(diphenylphosphino)benzaldehyde with aniline. The following metalation of **1** with $MnBr(CO)_5$, $FeBr_2$, and $CoCl_2$ afforded complexes **1-Mn**, **1-Fe**, and **1-Co**, respectively. The obtained complexes were fully characterized, including X-ray diffraction analysis. Complex **1-Mn** is diamagnetic, and its $^{31}P\{^1H\}$-NMR spectrum in $CDCl_3$ showed a singlet at δ_P 37.9 ppm (δ_P 37.9 ppm in C_6D_6) for the coordinated PN^H ligand (*vs.* the ^{31}P-resonance at δ_P −15.3 ppm in $CDCl_3$ for free PN^H). The ^1H-NMR spectrum of **1-Mn** revealed a triplet for the N*H* resonance at δ_H 4.49 ppm (J = 10.9 Hz) and a doublet of doublets for the methylene group at δ_H 4.12 ppm (J = 3.3 Hz and 11.8 Hz). Three non-equivalent CO ligands of **1-Mn** gave rise to three resonances at δ_C 212.6 ppm (br d, J_{C-P} = 36.2 Hz), 222.7 ppm (br d, J_{C-P} = 21.9 Hz), and 223.3 ppm (br s) in its $^{13}C\{^1H\}$-NMR spectrum in $CDCl_3$. The presence of three CO ligands in **1-Mn** was also supported by the IR spectroscopy, which revealed C═O stretches at υ 1897, 1941, and 2023 cm^{-1}. The molecular structure of **1-Mn** obtained by single crystal X-ray analysis is shown in Fig. 1A, and the selected structural parameters for **1-Mn** are listed in Table 1. The complex adopts an octahedral geometry, stabilizing an 18e valence shell. The PN^H ligand and two CO ligands of **1-Mn** occupy equatorial positions, whereas the residual CO ligand and the bromide are located in apical positions, with the bromide and the NH moiety being *cis*- to each other. Overall, the structural parameters of **1-Mn** are similar to those previously reported for the related aminophosphine Mn(I) tricarbonyl bromide complexes.[6]

The reaction of the PN^H ligand **1** with $FeBr_2$ afforded a paramagnetic complex **1-Fe** (Scheme 2). The ^1H-NMR analysis of **1-Fe** revealed very broad and uninformative spectra, consistent with the paramagnetic nature of the complex. The magnetic moment of 5.3μ_B was determined for **1-Fe** by solution measurements using the Evans method,[7] which corresponds to a high-spin (S = 2) Fe(II) d^6 species having four unpaired electrons. This suggests a tetrahedral geometry of the complex, which was further supported by an X-ray diffraction analysis of single crystals obtained by slow diffusion of hexanes into a CH_2Cl_2 solution of **1-Fe** at room temperature. The molecular structure

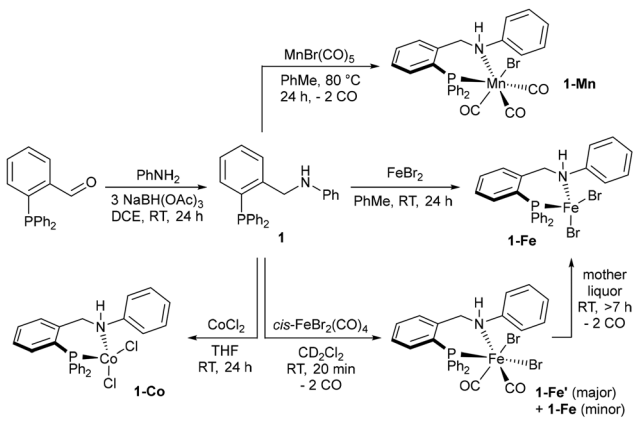

Scheme 2 Synthesis of PN^H complexes of Mn(I) (**1-Mn**), Fe(II) (**1-Fe**) and Co(II) (**1-Co**).

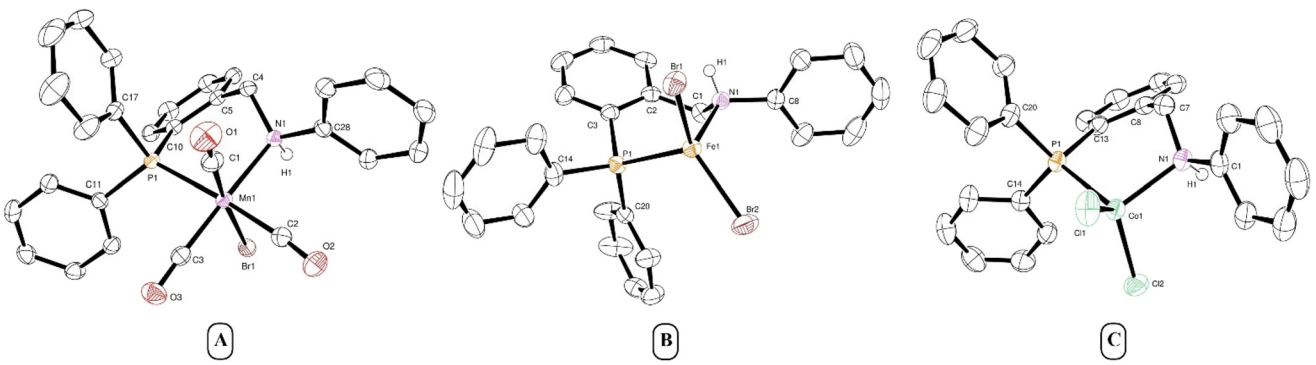

Fig. 1 Molecular structures of $(PN^H)MnBr(CO)_3$ (**1-Mn**; A), $(PN^H)FeBr_2$ (**1-Fe**; B), and $(PN^H)CoCl_2$ (**1-Co**; C), depicted with 50% thermal ellipsoids probability level (hydrogen atoms except for N–H are omitted for clarity). Selected bond distances (Å) and angles (°) are shown in Table 1.

Table 1 Selected bond distances (Å) and angles (°) for complexes **1-Mn**, **1-Fe**, and **1-Co**

$(PN^H)MnBr(CO)_3$ (**1-Mn**)			
Mn1–P1	2.3525(4)	P1–Mn1–N1	89.66(3)
Mn1–N1	2.1696(12)	C1–Mn1–Br1	175.06(5)
Mn1–Br1	2.5201(3)	C1–Mn1–N1	92.52(6)
Mn1–C1	1.7972(16)	C1–Mn1–C2	89.15(7)
Mn1–C2	1.8371(16)	C1–Mn1–C3	92.58(7)
Mn1–C3	1.7946(15)	C2–Mn1–C3	87.23(7)
P1–Mn1–C1	92.57(5)	C2–Mn1–N1	93.68(6)
P1–Mn1–C2	176.18(5)	C2–Mn1–Br1	87.00(5)
P1–Mn1–C3	89.28(5)	C3–Mn1–N1	174.83(6)
P1–Mn1–Br1	91.466(11)	C3–Mn1–Br1	90.31(5)
N1–Mn1–Br1	84.66(3)		
$(PN^H)FeBr_2$ (**1-Fe**)			
Fe1–P1	2.4558(7)	P1–Fe1–Br1	112.50(2)
Fe1–N1	2.171(2)	P1–Fe1–Br2	115.51(2)
Fe1–Br1	2.3812(4)	Br1–Fe1–Br2	117.941(17)
Fe1–Br2	2.3648(4)	Br1–Fe1–N1	102.42(6)
P1–Fe1–N1	89.36(6)	Br2–Fe1–N1	114.81(6)
$(PN^H)CoCl_2$ (**1-Co**)			
Co1–P1	2.3621(4)	P1–Co1–Cl1	110.288(16)
Co1–N1	2.0805(12)	P1–Co1–Cl2	109.769(17)
Co1–Cl1	2.1927(4)	Cl1–Co1–Cl2	121.003(19)
Co1–Cl2	2.2301(4)	Cl1–Co1–N1	108.42(4)
P1–Co1–N1	98.86(3)	Cl2–Co1–N1	106.11(4)

of **1-Fe** is depicted in Fig. 1 (selected structural parameters are listed in Table 1), showing a coordinatively unsaturated tetrahedral Fe(II) d^6 centre with one of the bromides pointing towards the NH moiety of the PN^H ligand. The structural parameters of **1-Fe**, including Fe–Br, Fe–N, and Fe–P bond distances, resemble those for the previously reported related phosphinopyridine, phosphinophenanthridine, phosphinoquinoline, and other κ^2-PN Fe(II) halides.[8]

Despite the coordinative unsaturation of **1-Fe**, no addition of CO to **1-Fe** to give a low-spin (S = 0) dicarbonyl derivative $(PN^H)FeBr_2(CO)_2$ was observed when the reaction of **1-Fe** with CO was performed in dichloromethane at room temperature. A similar poor reactivity with CO has been previously reported by Kirchner *et al.* for the related high-spin $(PN^{Py})FeBr_2$ complex (PN^{Py} = *N*-(diisopropylphosphino)pyridin-2-amine).[8a] In this case, in addition to the unfavorable entropy of the formation of $(PN^{Py})FeBr_2(CO)_2$ (coupled with the low solubility of CO), the more thermodynamically favorable product of CO addition, *cis*-CO,*trans*-Br-$(PN^{Py})FeBr_2(CO)_2$, was found to be kinetically labile and readily liberated CO at room temperature to recover the starting high-spin complex $(PN^{Py})FeBr_2$.

In contrast, the NMR scale reaction of the ligand **1** with *cis*-$FeBr_2(CO)_4$ [9] in CD_2Cl_2 resulted in 20 min at room temperature in a mixture of a paramagnetic complex **1-Fe** (minor component) and a diamagnetic low-spin (S = 0) carbonyl derivative **1-Fe′** assigned to *cis*-CO,*cis*-Br-$(PN^H)FeBr_2(CO)_2$ (major component; Scheme 2).[10] The latter species gave rise to a ^{31}P-resonance at δ_P 60.1 ppm (s) in its $^{31}P\{^1H\}$-NMR spectrum and characteristic ^1H-NMR resonances at δ_H 4.39 ppm (br d, J = 12.1 Hz), 4.92 ppm (d, J = 12.9 Hz) and 5.85 ppm (br s) for the diastereotopic methylene protons and the NH moiety of the coordinated PN^H ligand, respectively. The *cis*-CO,*cis*-Br structure of **1-Fe′** with one CO ligand being *trans*- to the amine donor of the PN^H ligand and another CO being *trans*- to the bromide was suggested based on the ligand field considerations and is consistent with the analogous *cis*-CO,*cis*-Br-$(PN^{Py})FeBr_2(CO)_2$ complex, previously reported by Kirchner *et al.* and produced by the reaction of *cis*-$FeBr_2(CO)_4$ with the PN^{Py} ligand.[8a] However, in contrast to Kirchner's *cis*-CO,*cis*-Br-$(PN^{Py})FeBr_2(CO)_2$, **1-Fe′** turned out to be unstable in solution at room temperature showing >90% decomposition within 7 h (approx. 50% decomposition of **1-Fe′** was observed in 2 h at room temperature in CD_2Cl_2)[10] presumably *via* the release of CO to give **1-Fe** (Scheme 2). Due to the instability of **1-Fe′** and rather long $^{13}C\{^1H\}$-NMR acquisition times, all attempts to observe ^{13}C-resonances for CO ligands of **1-Fe′** were unsuccessful. Nonetheless, freshly generated **1-Fe′** was subjected to the IR analysis in CD_2Cl_2, which revealed two characteristic stretches at υ 2002 cm^{-1} and 2050 cm^{-1} for two non-equivalent CO ligands, suggesting a *cis*-dicarbonyl structure of the complex.[8a]

Density functional theory (DFT)[11] studies were conducted to gain a better understanding of the thermodynamic stability of **1-Fe′** and its decomposition pathway to the high-spin low-coordinate **1-Fe** derivative. The stability of **1-Fe′** relative to the tetracoordinate complex **1-Fe** (was set as 0.0 kcal mol^{-1}) was evaluated by calculating the Gibbs free energy of the reaction of **1-Fe** with CO in CH_2Cl_2 using PBE0-D3BJ/def2-TZVPP//M06-L/def2-SVP.[12–16] In agreement with the experimental results (*vide supra*), these studies revealed that **1-Fe′** is by 13.1 kcal mol^{-1} less stable compared to **1-Fe**. The decomposition of **1-Fe′** to **1-Fe** is likely initiated by the endergonic (by 3.5 kcal mol^{-1}) singlet to quintet spin state change with an associated barrier of 13.6 kcal mol^{-1}, followed by the low barrier (1.2–2.4 kcal mol^{-1}) CO release to produce **1-Fe**.[10]

Analogously to iron, the reaction of the aminophosphine PN^H ligand **1** with $CoCl_2$ in THF at room temperature resulted in a paramagnetic complex **1-Co** (Scheme 2). Similar to **1-Fe**, the NMR analysis of **1-Co** revealed very broad and uninformative spectra consistent with the paramagnetic nature of the complex. The magnetic moment for **1-Co** was determined by Evans method[7] and was found to be 4.19μ_B, suggesting the presence of a high-spin Co(II) d^7 centre with three unpaired electrons. The X-ray diffraction analysis of the single crystals of **1-Co** obtained from its CH_2Cl_2 solution at −30 °C revealed a coordinatively unsaturated tetrahedral Co(II) complex (Fig. 1), structural parameters of which are similar to those for **1-Fe** (Table 1). By analogy with **1-Co**, a closely related iminophosphine derivative $(PN^{DMP})CoCl_2$ (**2-Co**; DMP = 2,6-dimethylphenyl) was obtained by the treatment of $CoCl_2$ with the PN^{DMP} ligand **2** in THF (Scheme 3). The single crystal X-ray diffraction analysis of **2-Co** also revealed an unsaturated tetrahedral structure of the complex (Fig. 2). Moreover, to compare the catalytic performance of the secondary aminophosphine PN^H ligand **1** with its tertiary aminophosphine counterpart, the PN^{Me2} ligand **3** was also prepared from 2- (diphenylphosphino)benzaldehyde (Scheme 3).

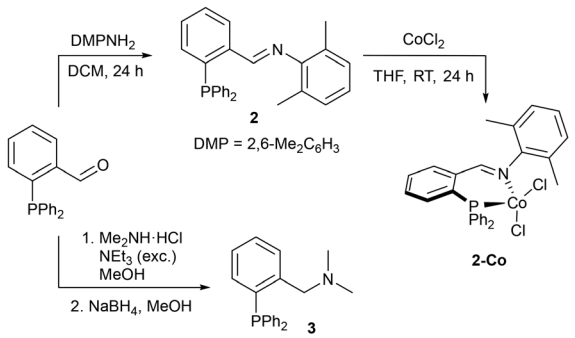

Scheme 3 Synthesis of ligands **2** and **3**, and the iminophosphine complex **2-Co**.

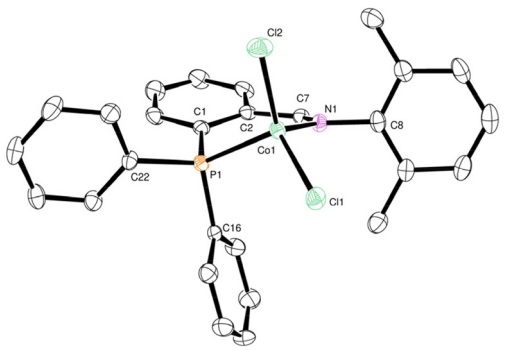

Fig. 2 Molecular structure of (PN^{DMP})$CoCl_2$ (**2-Co**), depicted with 50% thermal ellipsoids probability level (hydrogen atoms are omitted for clarity). Selected bond distances (Å): Co1–P1 2.3313(6), Co1–N1 2.0416 (19), Co1–Cl1 2.2177(6), Co1–Cl2 2.2118(7). Selected bond angles (°): P1–Co1–N1 91.82(5), P1–Co1–Cl1 110.70(2), P1–Co1–Cl2 112.12(3), Cl1–Co1–Cl2 113.87(3), Cl1–Co1–N1 111.16(6), Cl2–Co1–N1 115.19(6).

Catalytic transfer hydrogenation of nitriles

Having a series of aminophosphine PN^H complexes of Mn(I), Fe(II), and Co(II) in hands, we then tested their catalytic activities in the TH of nitriles with ammonia borane (NH_3BH_3; AB) as the hydrogen source. Compared to alcohols, which are typically employed in the TH of carbonyl compounds,[1,3] the use of AB in the TH of nitriles eliminates the necessity of a base co-catalyst[1] and prevents possible amine-carbonyl condensation side-reactions, expected for transformations in alcohol media.[17] To compare the catalytic activities of the prepared complexes, PhCN was chosen as a model substrate, and the results of these catalytic trials are shown in Table 2. The reactions were performed in the presence of 5 mol% of pre-catalysts using 3 equiv. of AB. Based on the literature precedents,[4] three solvents, toluene, hexanes, and 2-propanol, were chosen as reaction media. Depending on the solvent, the conversion of PhCN was determined by ^{1}H-NMR using mesitylene as an internal standard, followed by quenching the reaction mixtures with MeOH and HCl. The yield of the resulting benzylammonium chloride (**4**) was determined by ^{1}H-NMR in D_2O using NaOAc as an internal standard. Notably, very low conversions of PhCN (max. 7%) were observed under catalyst-free conditions (entries 1, 5, 9, and 10). In contrast, catalytic reactions in PhMe at 60 °C using **1-Mn**, **1-Fe**, and **1-Co** selectively afforded benzylamine products (entries 2–4). Among all tested complexes, **1-Fe** proved the most effective providing >99% conversion of PhCN in 24 h at 60 °C with 94% yield of the benzylammonium salt (entry 3). Pre-catalysts **1-Mn** and **1-Co** afforded 64% and 60% of $BnNH_3Cl$ (Bn = benzyl), respectively (entries 2 and 4). For **1-Co**, trace amounts of dibenzylamine hydrochloride were also detected by ^{1}H-NMR.

Table 2 Evaluation of catalytic activities of aminophosphine complexes of Mn(I), Fe(II), and Co(II) in TH of PhCN with AB[a]

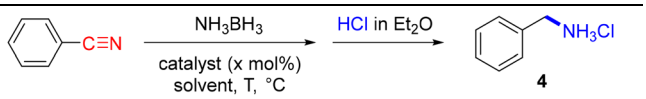

Entry	Cat. (mol%)	Solvent	T, °C/t, h	Conv.,[b] %	Yield,[c] %
1	—	PhMe	60/24	ND[d]	3
2	**1-Mn** (5)	PhMe	60/24	ND[d]	64
3	**1-Fe (5)**	**PhMe**	**60/24**	**>99**	**94**
4	**1-Co** (5)	PhMe	60/24	62	60
5	—	Hex	60/24	ND[d]	2
6	**1-Mn** (5)	Hex	60/24	ND[d]	62
7	**1-Fe (5)**	**Hex**	**60/24**	**>99**	**97**[e]
8	**1-Co** (5)	Hex	60/24	>99	85
9	**2-Co** (5)	Hex	60/24	>99	81
10	—	^{i}PrOH	80/24	ND[d]	7
11	—	^{i}PrOH	60/24	ND[d]	6
12	**1-Mn** (5)	^{i}PrOH	80/24	45	14[f]
13	**1-Fe** (5)	^{i}PrOH	80/24	0	0
14	**1-Co** (5)	^{i}PrOH	80/24	ND[d]	25[g]

[a] Conditions: PhCN (0.24 mmol), AB (0.72 mmol; 3 equiv.), C = 0.12 mol L^{-1}. [b] Determined by ^{1}H-NMR in the presence of mesitylene as an internal standard. [c] Reactions were quenched with MeOH and then with HCl. NMR yields of benzylammonium chloride (**4**) in D_2O were determined using NaOAc as an internal standard. [d] ND = not determined. [e] 12% with 1 mol% of **1-Fe** (24 h, 60 °C); 3% at 25 °C (24 h, 5 mol% of **1-Fe**); 54% when the reaction was conducted for 6 h (5 mol% of **1-Fe**, 60 °C). [f] 10% of Bn_2NH_2Cl were also detected by ^{1}H-NMR. [g] 17% of Bn_2NH_2Cl were also detected by ^{1}H-NMR.

In less polar hexanes, **1-Mn** revealed a similar catalytic activity compared to the reaction in PhMe (entry 6 *vs.* entry 2); whereas complexes **1-Fe** and **1-Co** proved more effective affording 97% and 85% of $BnNH_3Cl$ in 24 h at 60 °C, respectively (entries 7 and 8). Noteworthy, lowering the loading of **1-Fe** to 1 mol%, reducing the reaction time to 6 h, or reducing the reaction temperature to 25 °C resulted in significantly lower yields of benzylamine hydrochloride (max. 54%).

Interestingly, the iminophosphine derivative **2-Co** was also active in the TH of PhCN with AB in hexanes, showing an 81% yield of $BnNH_3Cl$ (entry 9 *vs.* 85% for the **1-Co**-catalyzed reaction in entry 8). This result coupled with a lack of the reactivity for tertiary aminophosphine ligand **3** (*vide infra*) suggests a possible *in situ* hydrogenation of the imino moiety of **2-Co** to a corresponding secondary aminophosphine derivative under TH conditions. Similar hydrogenation of iminopyridine ligands in Ru complexes has been previously reported by Keith and Chianese *et al.*[18]

On the other hand, the reduction of PhCN in 2-propanol was found to be sluggish and afforded only max. 25% of

$BnNH_3Cl$ (entries 12–14 for **1-Mn**, **1-Fe**, and **1-Co**, respectively). Moreover, in 2-propanol, the reactions were found to be less selective resulting in mixtures of $BnNH_3Cl$ with the secondary amine derivative, Bn_2NH_2Cl (entries 11 and 13).

Encouraged by the high catalytic activity of **1-Fe** as the first example of an iron system for TH of nitriles, we further explored the scope of nitrile substrates in **1-Fe**-catalyzed TH reactions (Scheme 4). To our delight, the system was found to be compatible with both electron-rich (**5**, **6**, **14**) and electron-deficient (**7**–**13**) aromatic nitriles, as well as with aliphatic substrates (**15**–**17**), selectively affording the corresponding hydrochloride salts of primary amine products. Among 4-halobenzonitriles (**7**–**9**), the 4-bromosubstituted derivative showed the lowest conversion of the substrate (40%) and afforded only 10% of 4-Br-$C_6H_4CH_2NH_3Cl$ (**9**) suggesting catalyst deactivation *via* C–Br bond cleavage.[19] The **1-Fe**-catalyzed TH of methyl 4-cyanobenzoate, 4-cyano-*N*,*N*-dimethylbenzamide and 2-cyanothiophene was found to be chemoselective, albeit required elevated temperatures (100 °C) for completion (**11**–**13** in Scheme 4). In contrast, the TH of 4-nitrobenzonitrile with AB turned out to be not selective and afforded only 21% of the desired 4-nitrobenzylamine hydrochloride (**14**) in a mixture with products of the nitro group reduction. Increasing the concentration of AB in the reduction of 4-nitrobenzonitrile resulted in 64% of *p*-$ClH_3NC_6H_4CH_2NH_3Cl$ as a product of the complete reduction of both cyano and nitro groups (20% of 4-nitrobenzylamine hydrochloride (**14**) were detected by ^{1}H-NMR). Despite the lack of nitro *vs.* nitrile selectivity, these observations suggest that **1-Fe** could be also utilized in the TH of nitro compounds.[20] Such reactions are currently under investigation in our laboratories and will be reported in due course.

Generally, compared to benzonitriles, the **1-Fe**-catalyzed TH of aliphatic nitriles required more forcing conditions (100 °C, 24 h); however, almost quantitative conversions of the substrates and good yields of the corresponding primary ammonium salts were observed (**15**–**18**; Scheme 4). In no case, the formation of secondary amine derivatives was detected. Notably, similar to 4-nitrobenzonitrile, the **1-Fe**-catalyzed TH of *E*-cinnamonitrile was found to be non-chemoselective. At 60 °C with 3 equiv. of AB, only 29% of the corresponding hydrochloride salt **16** was detected, along with 28% of the fully reduced product, 3-phenylpropylamine hydrochloride **17**. Increasing the temperature of the reaction to 100 °C resulted in the formation of 63% of **17**. A similar yield of **17** (69%) was also observed when the reaction was conducted with 4 equiv. of AB for 24 h at 100 °C (Scheme 4).

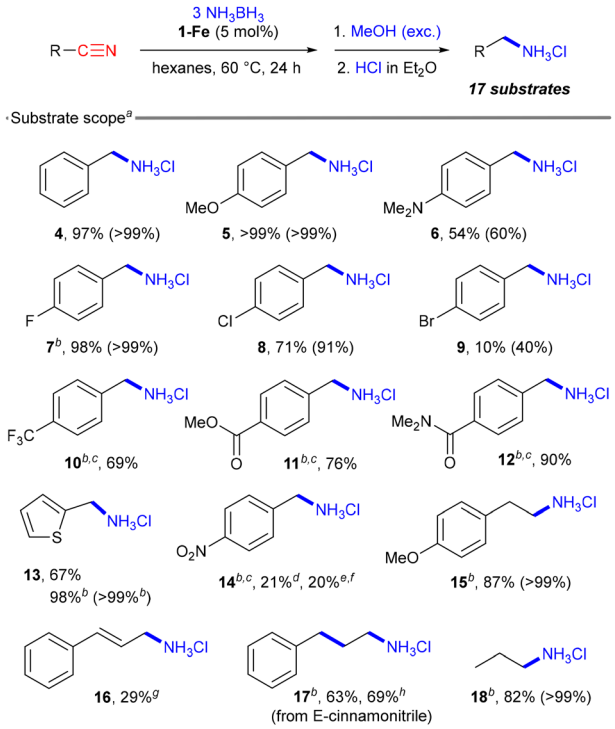

Scheme 4 Scope of **1-Fe**-catalyzed transfer hydrogenation of nitriles. [a] Conditions: nitrile (0.24 mmol), AB (0.72 mmol), C = 0.12 mol L^{-1}. Yields of hydrochloride salts after quenching the reactions mixtures with MeOH and then with HCl are shown (see the ESI† for details), determined by ^{1}H-NMR in D_2O using NaOAc as an internal standard. Conv. of nitriles are shown in parentheses, determined by ^{1}H-NMR taken directly from reaction mixtures using mesitylene as an internal standard. [b] 100 °C, 24 h. [c] Conv. was not determined due to the partial solubility of substrates in hexanes. [d] 48% of hydrochloride salts resulting from partial/complete reduction of the nitro group were detected. [e] 64% of the product of complete reduction of both CN and NO_2 groups of the substrate (*p*-ClH_3N-C_6H_4-CH_2NH_3Cl) was observed. [f] 6 equiv. of AB were used. [g] 28% of 3-phenylpropylamine hydrochloride was detected. [h] With 4 equiv. of AB.

Mechanistic aspects of transfer hydrogenation reactions

To shed some light on the mechanism of TH reactions, we performed a series of control experiments as well as DFT calculations[11] of the **1-Fe**-catalyzed reduction of PhCN with AB. First, the release of H_2 from AB in the presence of 5 mol% of **1-Fe** was observed by the ^{1}H-NMR spectroscopy (δ_H 4.47 ppm in C_6D_6 [21]).[10] Second, considering the paramagnetic nature of **1-Fe**, the possibility of the generation of a metal hydride species was tested by the treatment of the structurally related diamagnetic **1-Mn** derivative with AB and $LiBHEt_3$ (Scheme 5a). The stoichiometric reaction of **1-Mn** with AB in C_6D_6 was monitored by NMR (Fig. S24 and S25 in the ESI†). Immediately after mixing **1-Mn** and AB, the formation of H_2 was observed in the ^{1}H-NMR spectrum. Leaving the reaction mixture for 18 h resulted in further H_2 release and the formation of trace amounts of several hydride species, the major of which was tentatively assigned to $(PN^H)Mn(H)(CO)_3$ (**1-MnH**) and characterized by the upfield ^{1}H resonance at δ_H −6.97 ppm (doublet) with a $^2J_{H-P}$ coupling constant of 33.9 Hz. The small value of the observed $^2J_{H-P}$ coupling constant suggested a mutually *cis*-arrangement of the Mn-bound hydride and the phosphine arm of the coordinated PN^H ligand in **1-MnH**. The subsequent heating of this sample at 60 °C for 6 h revealed the generation of small amounts of another hydride species (δ_H = −7.61 ppm, broad singlet) and the formation of μ-aminodiborane (ADB; δ_B = −27.5 ppm) and bora-

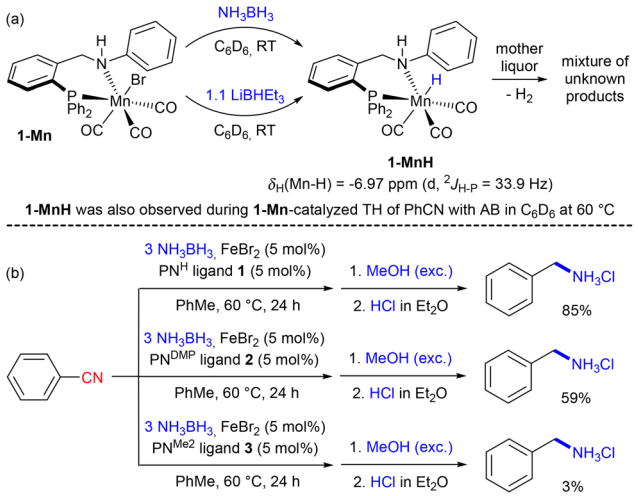

Scheme 5 Mechanistic control experiments.

zine ($B_3N_3H_6$; δ_B = 29.9 ppm) as products of dehydrogenation of AB.[22]

Analogously, the room temperature reaction of **1-Mn** with $LiBHEt_3$ in C_6D_6 was monitored by NMR for 21 h (Fig. S26 and S27 in the ESI†). Immediately after mixing, the release of H_2 was observed giving rise to a characteristic resonance at δ_H 4.47 ppm in the ^{1}H-NMR spectrum.[21] Similarly to the reaction with AB, the formation of several hydride species was detected within 6 h at room temperature. However, compared to the reaction of **1-Mn** with AB, the major product herein gave rise to a slightly downfield shifted hydride resonance at δ_H −3.93 ppm (d, $^2J_{H-P}$ = 59.1 Hz) in the ^{1}H-NMR spectrum, coupled to the ^{31}P-resonance at δ_P 63.1 ppm in the $^{31}P\{^1H\}$-NMR spectrum. Interestingly, the initial formation of trace amounts of the same hydride complex was also seen in the ^{1}H-NMR spectrum taken from the reaction of **1-Mn** with AB after 6 h at room temperature; however, unlike in the reaction of **1-Mn** with $LiBHEt_3$, this species was not the major hydride product (Fig. S24 and S26 in the ESI†). Leaving the reaction of **1-Mn** with $LiBHEt_3$ for 21 h at room temperature and releasing the H_2 pressure resulted in the generation of the hydride complex **1-MnH** (δ_H 6.97 ppm, d, $^2J_{H-P}$ = 33.9 Hz), previously observed upon the treatment of **1-Mn** with AB (*vide supra*). Notably, the decomposition process *via* the release of the PN^H ligand was also suggested based on the $^{31}P\{^1H\}$-NMR analysis of the reaction mixture (Fig. S27 in ESI†). Interestingly, the formation of **1-MnH** was also detected in the ^{1}H-NMR spectra recorded directly from the reaction mixture during **1-Mn**-catalyzed TH of PhCN with AB in C_6D_6 at 60 °C (Fig. S28 in the ESI†), suggesting the intermediacy of the hydride species in the TH catalysis.

To get some insights into the role of the aminophosphine ligands, three comparative experiments were conducted for the Fe-catalyzed reduction of PhCN with 3 equiv. of AB in the presence of PN^H (**1**), PN^{DMP} (**2**) and PN^{Me2} (**3**) ligands (Scheme 5b). The iron bromide pre-catalysts were generated *in situ* from $FeBr_2$ and the corresponding ligand (**1**, **2** or **3**). Thus, the addition of AB to PhCN in the presence of 5 mol% of $FeBr_2$ and 5 mol% of the ligand **1** in PhMe resulted after 24 h at 60 °C in 85% of benzylamine hydrochloride **4**. These observations correlate well with the previously discussed catalytic activity of **1-Fe** (Table 1, entry 3). Replacing ligand **1** with the iminophosphine ligand **2** resulted in 59% of $BnNH_3Cl$. On the other hand, the analogous reduction of PhCN with AB using 5 mol% of $FeBr_2$ and 5 mol% of the PN^{Me2} ligand **3** afforded only about 3% of $BnNH_3Cl$. Such a drastic difference in the reactivity of the secondary aminophosphine ligand **1** *vs.* the tertiary aminophosphine ligand **3** suggests that the acidic NH proton in the amine arm of the ligand is crucial for catalytic turnover. For iminophosphine derivative **2**, which showed intermediate activity compared to ligands **1** and **3**, the *in situ* reduction of the imine group to the corresponding secondary amine functionality could be suggested, and similar transformations have been previously documented in the literature.[18] Likely, the TH reactions proceed *via* a metal–ligand cooperative pathway that involves the NH proton transfer from the PN^H ligand and the formation of the metal amide species (Scheme 6).[1h,i,k] Moreover, poor catalytic turnover observed for the tertiary aminophosphine ligand **3** could also rule out possible metal-centered hydroboration routes[23] and the routes that involve a proton transfer from AB.[4d,24]

To test possible inner-sphere (a stepwise hydride and proton transfer route A; Scheme 6) *vs.* outer-sphere (a concerted route B; Scheme 6) pathways[4c] of the **1-Fe**-catalyzed TH we turned to DFT calculations[11] of the **1-Fe**-catalyzed reduction of PhCN with AB. Geometries were optimized using the M06-L functional[12] and the def2-SVP basis set,[13] followed by single-point calculations performed at the PBE0-D3BJ/def2-TZVPP theory level.[13–16] Based on experimental observations for the reaction of the related **1-Mn** with AB (*vide supra*) and the literature precedents for activation of metal halide pre-catalysts with AB to generate a catalytically active metal hydride species,[4c,25] the reaction of **1-Fe** with AB likely produces the hydride catalyst akin to **1-FeH** in Scheme 6.[26] In the inner-sphere mechanism, considering the unsaturated nature of **1-FeH**, the coordination of PhCN to the iron centre can generate the intermediate **Int-1**, and this process was found to be endergonic by 4.8 kcal mol^{-1} (route A, Scheme 6). The subsequent migratory insertion of the nitrile into the Fe–H bond of **Int-1** to generate the imido intermediate **Int-2** has an associated barrier of 12.4 kcal mol^{-1} (**TS-1**) but was determined to be exergonic by 13.6 kcal mol^{-1}. **Int-2** can then undergo a proton transfer from the PN^H ligand to the imide substituent (see **TS-2**, 11.4 kcal mol^{-1}), affording an imine and an iron amide intermediate **Int-3**. This process turned out to be slightly endergonic by 5.1 kcal mol^{-1}. The overall barrier for the inner-sphere reduction of PhCN to the imine intermediate was calculated to be 17.2 kcal mol^{-1}; however, a slightly lower Gibbs free energy barrier of 12.7 kcal mol^{-1} was observed using M06-L/def2-SVP.[10]

Despite the coordinative unsaturation of **1-FeH**, the outer-sphere mechanism of the reduction of PhCN (route B, Scheme 6) to PhCH=NH seems somewhat more favorable, showing a barrier of 11.6 kcal mol^{-1} (10.6 kcal mol^{-1} using

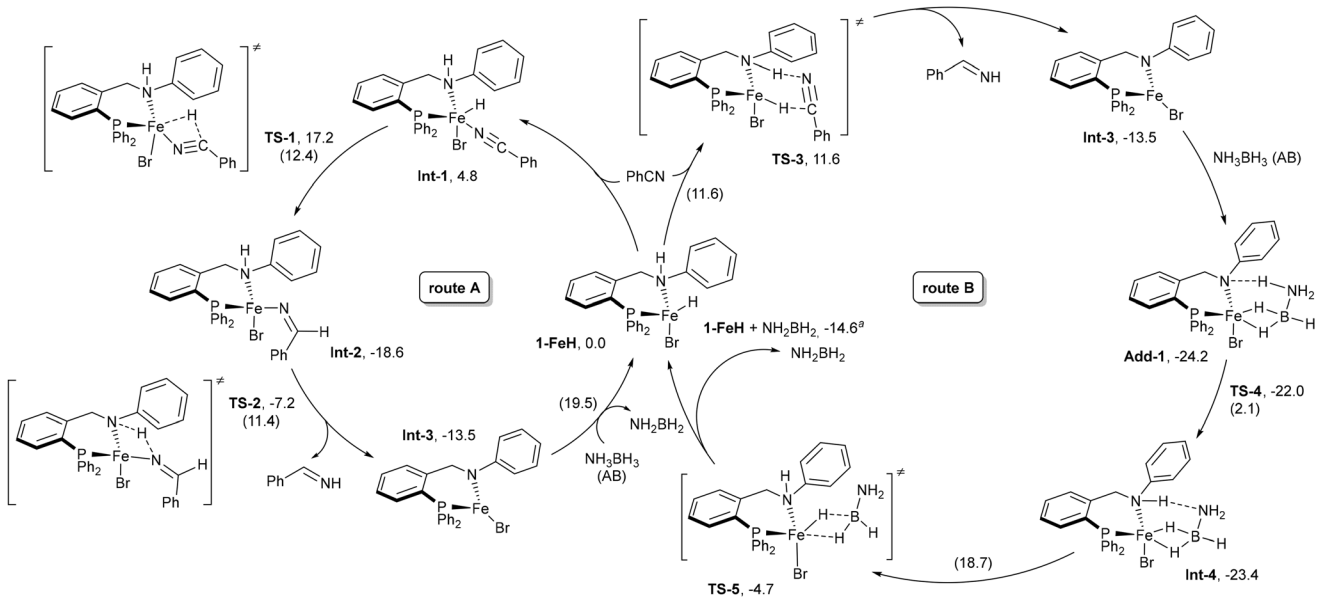

Scheme 6 DFT-derived plausible mechanism for **1-Fe**-catalyzed TH of PhCN with AB (PBE0-D3BJ/def2-TZVPP//M06-L/def2-SVP in toluene; Gibbs free energies are shown in kcal mol^{-1}; values in parentheses reflect Gibbs free energy barriers). [a] The value of −14.6 kcal mol^{-1} is the calculated Gibbs free energy for the overall reaction of PhCN with AB to produce PhCH═NH and NH_2BH_2.

M06-L/def2-SVP; compared to 17.2 kcal mol^{-1} using PBE0-D3BJ/def2-TZVPP and 12.7 kcal mol^{-1} using M06-L/def2-SVP for the inner sphere pathway) with an asymmetric concerted transition state **TS-3**. However, the observed energy values difference for the inner- *vs.* outer-sphere routes does not allow for complete differentiation between the two possible reaction pathways, and both mechanisms seem possible under the applied reaction conditions (≥60 °C, 24 h; Scheme 4). Notably, a small difference in barriers for inner- and outer-sphere mechanisms is in line with our previous findings that **1-Fe** is more stable than the coordinatively saturated **1-Fe′** (Scheme S1†). Moreover, both routes presented in Scheme 6 share the same catalyst regeneration step by the dehydrogenation of AB with an amide intermediate **Int-3**. This latter transformation was found to be practically thermoneutral but showed the highest Gibbs free energy barrier of 19.5 kcal mol^{-1} (20.7 kcal mol^{-1} using M06-L/def2-SVP[10]). Interestingly, the dehydrogenation of AB was also suggested to proceed *via* an outer-sphere pathway (see route B in Scheme 6);[27] although, a highly asynchronous transfer of the proton and the hydride to nitrogen and iron, respectively, was found, with the highest transition state **TS-5** and a barrier of 18.7 kcal mol^{-1} being associated with the release of NH_2BH_2 from a low energy borohydride intermediate **Int-4**.

After the first hydrogen transfer cycle (Scheme 6), the produced primary imine intermediate PhC(H)═NH can be reduced to benzylamine *via* analogous mechanisms, or in a catalyst-free fashion. The possibility of the catalyst-free reaction was tested in the reduction of *N*-benzylideneaniline with 2 equiv. of AB, showing a 25% yield of *N*-benzylaniline hydrochloride under both **1-Fe**-catalyzed and catalyst-free conditions.[10] Based on these observations and considering a well-known greater reactivity of primary *vs.* secondary imines, one could suggest that the reduction of PhC(H)═NH with AB may not necessarily require the catalyst.

Conclusions

In summary, a series of aminophosphine PN^H complexes of Mn(I) (**1-Mn**), Fe(II) (**1-Fe**), and Co(II) (**1-Co**) were prepared and tested as pre-catalysts in the reduction of nitriles with AB. Among all investigated systems, the iron complex **1-Fe** showed the greatest catalytic activity, presenting the first example of an iron catalyst for TH of nitriles and a rare example of an iron TH catalyst beyond the reduction of carbonyl compounds. The system was found applicable to a wide scope of substrates, including aromatic and aliphatic derivatives, selectively affording primary amines and tolerating ester, carboxamide, and thiophene functionalities. Based on a series of control experiments as well as DFT calculations, the **1-Fe**-catalyzed TH of nitriles was suggested to proceed *via* a hydride metal–ligand cooperative mechanism, enabled by the NH proton transfer from the secondary aminophosphine PN^H ligand. Further studies of the catalytic activity of **1-Fe** in the TH of other unsaturated N-containing organic molecules (such as nitro compounds, N-heteroarenes, *etc.*) are currently undergoing in our laboratories.

Experimental section

General experimental methods, complete experimental, spectroscopic, computational details, and crystallographic data for

1-Mn, **1-Fe**, **1-Co**, and **2-Co** are described in the ESI.† *cis*-$FeBr_2(CO)_4$ [9] and the iminophosphine PN^{DMP} ligand **2** [28] were prepared according to the literature procedures.

Preparation of PN^H ligand 1

2-(Diphenylphosphino)benzaldehyde (1 g, 3.44 mmol), aniline (336 mg, 3.61 mmol), and $NaBH(OAc)_3$ (2.18 g, 10.32 mmol) were mixed in dichloroethane (DCE) (80 mL), and the resulting mixture was stirred at room temperature for 24 h. After the reaction was completed, 40 mL of saturated $NaHCO_3$ solution was added portionwise to the mixture. The solvent was evaporated, 25 mL of degassed water was added, and the product was extracted with CH_2Cl_2 (3 × 7 mL). The organic fraction was collected and dried over Na_2SO_4. The solvent was pumped off resulting in a white solid product, which was dried in vacuum (677.4 mg, 64%). ^{1}H-NMR (500 MHz; $CDCl_3$; δ, ppm): 7.51–7.48 (m, 1 H, aromatic); 7.39–7.27 (m, 11 H, aromatic); 7.19 (t, J = 7.4 Hz, 1 H, aromatic); 7.10 (t, J = 7.8 Hz, 2 H, aromatic); 6.95–6.91 (m, 1 H, aromatic); 6.67 (t, J = 7.3 Hz, 1 H, aromatic); 6.41 (d, J = 8.1 Hz, 2 H, aromatic); 4.50 (s, 2 H, *CH*$_2$N(H)Ph); 3.94 (br s, 1 H, *NH*). ^{13}C{^{1}H}-NMR (126 MHz; $CDCl_3$; δ, ppm): 147.8 (s); 143.4 (d, J = 23.1 Hz); 136.4 (d, J = 9.7 Hz); 135.9 (d, J = 14.9 Hz); 134.1 (d, J = 19.8 Hz); 133.7 (s); 129.21 (s); 129.18 (s); 129.0 (s); 128.8 (d, J = 7.1 Hz); 128.3 (d, J = 5.3 Hz); 127.6 (s); 117.5 (s); 113.0 (s); 47.0 (d, J = 23.4 Hz); ^{31}P{^{1}H}-NMR (202.5 MHz; $CDCl_3$; δ, ppm): −15.3 (s, 1 P, *P*Ph$_2$). NMR data are consistent with those previously reported in the literature.[29]

Preparation of PN^{Me2} ligand 3

$[Me_2NH_2]Cl$ (252.8 mg, 3.10 mmol) and NEt_3 (432 μL, 3.10 mmol) were added one by one at room temperature to a solution of 2-(diphenylphosphino)benzaldehyde (300 mg, 1.03 mmol) in 5 mL of MeOH. The reaction mixture was stirred overnight at room temperature forming a yellow suspension. The mixture was cooled to −5 °C, and $NaBH_4$ (101.6 mg, 2.69 mmol) was added portionwise during 1 h. When the addition of $NaBH_4$ was complete, the reaction was stirred at room temperature overnight. The solvent was pumped off; the residue was redissolved in 25 mL of benzene and filtered through a short column of silica gel. Removal of benzene in vacuum yielded a yellowish oil of ligand **3** (151.3 mg, 46%). ^{1}H-NMR (500 MHz; $CDCl_3$; δ, ppm): 7.44–7.46 (m, 1 H, aromatic); 7.28–7.33 (m, 7 H, aromatic); 7.22–7.27 (m, 4 H, aromatic); 7.14 (t, J = 7.5 Hz, 1 H, aromatic); 6.86–6.92 (m, 1 H, aromatic); 3.60 (s, 2 H, *CH*$_2$NMe$_2$), 2.06 (s, 6 H, N*Me*$_2$). ^{31}P{^{1}H}-NMR (202.5 MHz; $CDCl_3$; δ, ppm): −14.77 (s, 1 P, *P*Ph$_2$). ^{13}C{^{1}H}-NMR (126 MHz; $CDCl_3$; δ, ppm): 144.2 (d, J = 22.2 Hz); 137.9 (d, J = 10.2 Hz); 136.8 (d, J = 15.2 Hz); 134.0 (s); 133.8 (s); 129.1 (d, J = 5.4 Hz); 128.7 (s); 128.5 (d, J = 6.9 Hz); 128.4 (s); 127.2 (s); 62.3 (d, J = 17.9 Hz); 44.8 (s). NMR data are consistent with those previously reported in the literature.[30]

Preparation of $(PN^H)MnBr(CO)_3$ (1-Mn)

A solution of ligand **1** (93.6 mg, 0.255 mmol) in 10 mL of PhMe was added at room temperature to $Mn(CO)_5Br$ (70.0 mg, 0.255 mmol) in 10 mL of PhMe. The resulting mixture was stirred at 80 °C for 24 h to give an orange suspension. The solvent was pumped off; the residue was dried in vacuum and recrystallized from CH_2Cl_2/hexanes to give an orange solid (106.3 mg, 71%). ^{1}H-NMR (500 MHz; C_6D_6; δ, ppm): 8.30 (br s, 2 H, aromatic); 7.30–7.36 (m, 2 H, aromatic); 6.86–7.10 (m, 13 H, aromatic); 6.78–6.82 (m, 1 H, aromatic); 6.56–6.61 (m, 1 H, aromatic); 5.02 (d, J = 10.1 Hz, 1 H); 4.23–4.33 (m, 1 H); 3.60 (dd, J = 12.0, 3.9 Hz, 1 H). ^{31}P{^{1}H}-NMR (202.5 MHz; C_6D_6; δ, ppm): 38.3 (s, 1 P, *P*Ph$_2$). ^{31}P{^{1}H}-NMR (202.5 MHz; $CDCl_3$; δ, ppm): 37.9 (s, 1 P, *P*Ph$_2$). ^{13}C{^{1}H}-NMR (126 MHz; $CDCl_3$; δ, ppm): 223.3 (br s, CO); 222.7 (br d, J = 21.9 Hz, CO); 212.6 (br d, J = 36.2 Hz, CO); 153.5 (s); 138.7 (d, J = 16.1 Hz); 136.1 (d, J = 9.7 Hz); 133.5 (s); 132.8 (d, J = 10.3 Hz); 131.7 (s); 131.41 (s); 131.37 (d, J = 6.3 Hz); 130.7 (s); 130.4 (d, J = 6.0 Hz); 129.8 (s); 129.1 (d, J = 9.3 Hz); 128.9 (d, J = 9.7 Hz); 121.5 (s); 118.6 (s); 59.8 (d, J = 10.7 Hz). IR (nujol; selected stretches, cm^{-1}): 1897 (CO), 1941 (CO), 2023 (CO). Elem. analysis (%): calcd for $C_{28}H_{22}BrMnNO_3P$: C 57.36, H 3.78, N 2.39; found: C: 57.26, H 3.48, N 2.77.

Preparation of $(PN^H)FeBr_2$ (1-Fe)

A solution of ligand **1** (136 mg, 0.37 mmol) in 20 mL of PhMe was added at room temperature to $FeBr_2$ (79.8 mg, 0.37 mmol) in 10 mL of PhMe. The resulting mixture was stirred at room temperature for 24 h, the solvent was pumped off to give a brown residue which was dried in vacuum and recrystallized from CH_2Cl_2/hexanes to give a brown solid (168.3 mg, 78%). The produced compound is paramagnetic, μ_{eff} = 5.3μ_B (determined by Evans method[7] in $CHCl_3$ with a $CDCl_3$ insert). Elem. analysis (%): calcd for $C_{25}H_{22}Br_2FeNP$: C 51.50, H 3.80, N 2.40; found: C: 51.11, H 4.17, N 2.19.

Preparation of $(PN^H)CoCl_2$ (1-Co)

A solution of ligand **1** (100 mg, 0.27 mmol) in 20 mL of THF was added at room temperature to anhydrous $CoCl_2$ (35.3 mg, 0.27 mmol). The resulting mixture was stirred at room temperature for 24 h. The solvent was pumped off; the blue residue was dried in vacuum and recrystallized from CH_2Cl_2/hexanes to give bright blue crystals of **1-Co** (57.1 mg, 42%). The produced compound is paramagnetic, μ_{eff} = 4.19μ_B (determined by Evans method[7] in $CHCl_3$ with a $CDCl_3$ insert). Elem. analysis (%): calcd for $C_{25}H_{22}Cl_2CoNP$: C 60.39, H 4.46, N 2.82; found: C: 60.02, H 4.77, N 3.01.

Preparation of $(PN^{DMP})CoCl_2$ (2-Co)

The reaction was done analogously to the preparation of **1-Co**. A yellow solution of ligand **2** (93.1 mg, 0.237 mmol) in 5 mL of THF was added at room temperature to anhydrous $CoCl_2$ (30.8 mg, 0.237 mmol). Immediately after mixing, the color of the mixture turned green and then, within 10 min of stirring at room temperature, to dark blue. The resulting mixture continued to stir at room temperature for 24 h. The solvent was pumped off; the obtained residue was dried in vacuum and recrystallized from CH_2Cl_2/hexanes to give blue crystals of **2-Co** (69.5 mg, 56%). Elem. analysis (%): calcd for $C_{27}H_{24}Cl_2CoNP$: C 61.97, H 4.62, N 2.68; found: C: 62.13, H 4.92, N 3.05.

General procedure for catalytic TH reactions

In a typical procedure, AB (22.2 mg, 0.72 mmol; 3 equiv. to the substrate) and the metal pre-catalyst (either **1-Mn**, **1-Fe** or **1-Co**) (0.012 mmol; 5 mol% to the substrate) were weighed in a 10 mL Supelco headspace vial. A nitrile substrate (0.24 mmol) in a corresponding solvent (PhMe, C_6D_6, hexanes, or ^{i}PrOH) was added to the vial to achieve a 0.12 mol L^{-1} reaction mixture. The vial was equipped with a magnetic stirring bar and sealed under argon with a magnetic screw cap having PTFE-faced butyl septa. Depending on the substrate and the solvent used, the resulting mixture was left with stirring for 24 h either at 60 °C, 80 °C, or 100 °C (oil bath). After the reaction completion, mesitylene (0.1–0.2 equiv. to the substrate) was added as an internal standard, and the mixture was transferred to an NMR tube and submitted for ^{1}H-NMR analysis. Conversions of substrates were calculated (where possible) by the integration of substrate resonances against those for mesitylene. Then, the reaction mixture was quenched with 5 mL of MeOH (5 mL; 3 h of stirring at room temperature) (this step was omitted for reactions performed in ^{i}PrOH). The obtained methanol solution was filtered through a Celite pad, and the solvent was pumped off. The residue was dissolved in Et_2O (5 mL), and HCl (1 mL of a 1 M solution in Et_2O) was added. After continuous stirring for 3 h at room temperature, the formed precipitate was allowed to settle, the solvent was decanted, and the precipitate was washed with Et_2O (3 × 5 mL), dried in vacuum, weighed, and dissolved in D_2O. The resulting solution was submitted for NMR analysis using CH_3COONa (0.12 mmol) as an internal standard. Yields of the produced amine hydrochlorides were determined by ^{1}H-NMR. The reactions with lower/higher loadings of AB and/or the pre-catalyst and control experiment at lower temperatures and/or in the absence of a metal pre-catalyst were performed analogously. Conversions of substrates and yields of the hydrochloride salts can be found in Scheme 4. NMR data for amine hydrochlorides and the corresponding NMR spectra can be found in the ESI.†

Data availability

The data supporting this article have been included as part of the ESI.† Crystallographic data for **1-Mn**, **1-Fe**, **1-Co**, and **2-Co** have been deposited at the CCDC under 2379898, 2379897, 2380140, and 2379985† and can be obtained from **https://www.ccdc.cam.ac.uk**.

Conflicts of interest

There are no conflicts to declare.

Acknowledgements

This research work was funded by the Science Committee of the Ministry of Science and Higher Education of the Republic of Kazakhstan (project no. AP14870723 to A. Y. K.). The support from Nazarbayev University (FDCRG grant no. 201223FD8826 to A. Y. K.) is also acknowledged. We thank Alibek Nurseiit (NU) and Saniya Rakisheva (NU) for the preparation of **2-Co** and preliminary testing of the catalytic activity of **1-Mn**, respectively.

References

1 (*a*) R. Noyori and S. Hashiguchi, *Acc. Chem. Res.*, 1997, **30**, 97–102; (*b*) S. E. Clapham, A. Hadzovic and R. H. Morris, *Coord. Chem. Rev.*, 2004, **248**, 2201–2237; (*c*) K.-H. Fujita and R. Yamaguchi, *Synlett*, 2005, 560–571; (*d*) S. Gladiali and E. Alberico, *Chem. Soc. Rev.*, 2006, **35**, 226–236; (*e*) T. Ikariya and J. Blacker, *Acc. Chem. Res.*, 2007, **40**, 1300–1308; (*f*) R. H. Morris, *Chem. Soc. Rev.*, 2009, **38**, 2282–2291; (*g*) R. Malacea, R. Poli and E. Manoury, *Coord. Chem. Rev.*, 2010, **254**, 729–752; (*h*) P. E. Sues, K. Z. Demmans and R. H. Morris, *Dalton Trans.*, 2014, **43**, 7650–7667; (*i*) D. Wang and D. Astruc, *Chem. Rev.*, 2015, **115**, 6621–6686; (*j*) B. Štefane and F. Požgan, *Top. Curr. Chem.*, 2016, **374**, 18; (*k*) D. Baidilov, D. Hayrapetyan and A. Y. Khalimon, *Tetrahedron*, 2021, **98**, 132435and references therein.

2 (*a*) *The Handbook of Homogeneous Hydrogenation*, ed. J. G. de Vries and C. J. Elsevier, Wiley-VCH, Weinheim, 2007; (*b*) *Modern Reduction Methods*, ed. P. G. Andersson and I. J. Munslow, Wiley-VCH, Weinheim, 2008.

3 (*a*) A. Robertson, T. Matsumoto and S. Ogo, *Dalton Trans.*, 2011, **40**, 10304–10310; (*b*) F. Foubelo, C. Najera and M. Yus, *Tetrahedron: Asymmetry*, 2015, **26**, 769–790.

4 (*a*) Z. Shao, S. Fu, M. Wie, S. Zhou and Q. Liu, *Angew. Chem., Int. Ed.*, 2016, **55**, 14653–14657; (*b*) J. A. Garduño, M. Flores-Alamo and J. Garcia, *ChemCatChem*, 2019, **11**, 5330–5338; (*c*) K. Sarkar, K. Das, A. Kundu, D. Adhikari and B. Maji, *ACS Catal.*, 2021, **11**, 2786–2794; (*d*) S. Weber, I. Blaha and K. Kirchner, *Catal. Sci. Technol.*, 2024, **14**, 4843–4847.

5 (*a*) R. C. Larock, *Comprehensive Organic Transformations: A Guide to Functional Group Preparation*, Wiley, New York, 1989; (*b*) S. A. Lawrence, *Amines: Synthesis, Properties and Applications*, Cambridge University Press, Cambridge, 1st edn, 2004; (*c*) A. Ricci, in *Amino Group Chemistry, From Synthesis to Life Sciences*, ed. A. Ricci, Wiley-VCH, Weinheim, 2008.

6 For examples, see:(*a*) D. Wei, A. Bruneau-Voisine, T. Chauvin, V. Dorcet, T. Roisnel, D. A. Valyaev, N. Lugan and J.-B. Sortais, *Adv. Synth. Catal.*, 2018, **360**, 676–681; (*b*) V. Vigneswaran, S. N. MacMillan and D. C. Lacy, *Organometallics*, 2019, **38**, 4387–4391; (*c*) S. M. W. Rahaman, D. K. Pandey, O. Rivada-Wheelaghan, A. Dubey, R. R. Fayzullin and J. R. Khusnutdinova, *ChemCatChem*, 2020, **12**, 5912–5918; (*d*) K. Azouzi, A. Bruneau-Voisine, L. Vendier, J.-B. Sortais and S. Bastin, *Catal. Commun.*, 2020, **142**, 106040;

(*e*) Z. Császár, R. Kovács, M. Fonyó, J. Simon, A. Bényei, G. Lendvay, J. Bakos and G. Farkas, *Mol. Catal.*, 2022, **529**, 112531; (*f*) V. Vigneswaran, P. C. Abhyankar, S. N. MacMillan and D. C. Lacy, *Organometallics*, 2022, **41**, 67–75.

7 E. M. Schubert, *J. Chem. Educ.*, 1992, **69**, 62.

8 (*a*) C. Holzhacker, C. M. Standfest-Hauser, M. Puchberger, K. Mereiter, L. F. Veiros, M. J. Calhorda, M. D. Carvalho, L. P. Ferreira, M. Godinho, F. Hartl and K. Kirchner, *Organometallics*, 2011, **30**, 6587–6601; (*b*) S. Chakraborty, G. Leitus and D. Milstein, *Chem. Commun.*, 2016, **52**, 1812–1815; (*c*) R. Mondal, F. D. Braun, I. B. Lozada, R. Nickel, J. van Lierop and D. E. Herbert, *New J. Chem.*, 2021, **45**, 4427–4436; (*d*) P. Schlitz, N. Casaretto, S. Bourcier, A. Auffrant and C. Gosmini, *Dalton Trans.*, 2023, **52**, 14859–14866.

9 (*a*) W. Hieber and G. Bader, *Ber. Dtsch. Chem. Ges.*, 1928, **61**, 1717–1722; (*b*) E. W. Robertson, O. M. Wilkin and N. A. Young, *Polyhedron*, 2000, **19**, 1493–1502; (*c*) Z. Xiao, R. Jiang, J. Jin, X. Yang, B. Xu, X. Liu, Y. He and Y. He, *Dalton Trans.*, 2019, **48**, 468–477; (*d*) T. Čarný, P. Kisszékelyi, M. Markovič, T. Gracza, P. Kóóš and R. Šebesta, *Org. Lett.*, 2023, **25**, 8617–8621.

10 See the ESI† for details.

11 R. G. Parr and W. Yang, *Density Functional theory of Atoms and Molecules*, Oxford University Press, New York, 1989.

12 Y. Zhao and D. G. Truhlar, *J. Chem. Phys.*, 2006, **125**, 1–18.

13 J. P. Perdew, M. Ernzerhof and K. Burke, *J. Chem. Phys.*, 1996, **105**, 9982–9985.

14 C. Adamo and V. Barone, *J. Chem. Phys.*, 1999, **110**, 6158–6170.

15 F. Weigend and R. Ahlrichs, *Phys. Chem. Chem. Phys.*, 2005, **7**, 3297–3305.

16 S. Grimme, S. Ehrlich and L. Goerigk, *J. Comput. Chem.*, 2011, **32**, 1456–1465.

17 (*a*) J. Zhang, E. Balaraman, G. Leitus and D. Milstein, *Organometallics*, 2011, **30**, 5716–5724; (*b*) I. D. Alshakova, B. Gabidullin and G. I. Nikonov, *ChemCatChem*, 2018, **10**, 4860–4869.

18 T. He, J. C. Buttner, E. F. Reynolds, J. Pham, J. C. Malek, J. M. Keith and A. R. Chianese, *J. Am. Chem. Soc.*, 2019, **141**, 17404–17413.

19 For examples, see:(*a*) C. Chen, H. Zuo and K. S. Chan, *Tetrahedron*, 2019, **75**, 510–517; (*b*) M. Segizbayev, Ö. Öztopçu, D. Hayrapetyan, D. Shakhman, K. A. Lyssenko and A. Y. Khalimon, *Dalton Trans.*, 2020, **49**, 11950–11957; (*c*) X. Wen, Y. Gong, S. Niu, T. Luo, H. Xi and W. Liu, *Eur. J. Org. Chem.*, 2023, **26**, e202201376.

20 D. Formenti, F. Ferretti, F. K. Scharnagl and M. Beller, *Chem. Rev.*, 2019, **119**, 2611–2680.

21 G. R. Fulmer, A. J. M. Miller, N. H. Sherden, H. E. Gottlieb, A. Nudelman, B. M. Stoltz, J. E. Bercaw and K. I. Goldberg, *Organometallics*, 2010, **29**, 2176–2179.

22 A. Yessengazin, B. Seisenkul, S. Tussupbayev, T. Andizhanova and A. Y. Khalimon, *ChemCatChem*, 2024, e202400876.

23 D. Hayrapetyan and A. Y. Khalimon, *Chem. – Asian J.*, 2020, **15**, 2575–2587.

24 Z. Shao, S. Fu, M. Wie, S. Zhou and Q. Liu, *Angew. Chem., Int. Ed.*, 2016, **55**, 14653–14657.

25 For example:(*a*) S. Fu, N.-Y. Chen, X. Liu, Z. Shao, S.-P. Luo and Q. Liu, *J. Am. Chem. Soc.*, 2016, **138**, 8588–8594; (*b*) A. Brzozowska, L. M. Azofra, V. Zubar, I. Atodiresei, L. Cavallo, M. Rueping and O. El-Sepelgy, *ACS Catal.*, 2018, **8**, 4103–4109.

26 Although we can not completely rule out the formation of a borohydride complex akin to (PNH)Fe(Br)(BH_4), for **1-Mn**-catalyzed TH of PhCN, no such species was detected by NMR. Similar observations have been previously reported by Kirchner and Weber *et al.*, see ref. 4*d*.

27 Analogous concerted dehydrogenation of AB was also suggested by Adhikari and Maji *et al.* in the Mn-catalyzed TH of nitriles, see ref. 4*c*.

28 W. M. Motswainyana, M. O. Onani, A. M. Madiehe, M. Saibu, N. Thovhogi and R. A. Lalancette, *J. Inorg. Biochem.*, 2013, **129**, 112–118.

29 T. Traut-Johnstone, S. Kanyanda, F. H. Kriel, T. Viljoen, P. D. R. Kotze, W. E. van Zyl, J. Coates, D. J. G. Rees, M. Meyer, R. Hewer and D. B. G. Williams, *J. Inorg. Biochem.*, 2015, **145**, 108–120.

30 Y. Li, S. Chakrabarty, C. Mück-Lichtenfeld and A. Studer, *Angew. Chem., Int. Ed.*, 2016, **55**, 802–806.